7•8•2012

ЕЛЕКТРОТЕХНИКА И ЕЛЕКТРОНИКА

ELECTROTECHNICA & ELECTRONICA

E+E

UNIVERSITY OF NIŠ, SERBIA
FACULTY OF ELECTRONIC ENGINEERING

Celebrating half a century of existence, continuous lasting and permanent development

www.elfak.ni.ac.rs

Contact info: address: Aleksandra Medvedeva 14, 18000 Niš, Serbia |
phone: +381 (18) 529 105 | e-mail: efinfo@elfak.ni.ac.rs

ELEKTROTECHNICA & ELEKTRONICA E+E

Vol. 47. No 7-8/2012

Monthly scientific and technical journal

Published by:
The Union of Electronics, Electrical Engineering and Telecommunications /CEEC/, BULGARIA

Corresponding address:
PO Box 98
108 "Rakovski" str.
Sofia 1000
BULGARIA

Tel. +359 2 987 97 67
+359 2 988 01 98
e-mail: epluse@mail.bg
http://ceec.fnts.bg/sp-E+E.htm

ISSN 0861-4717

C O N T E N T S

ELECTRONICS

Dragana U. Živaljević, Vidosav S. Stojanović
Round-off noise calculation in power symmetric filterbank using parallel connection of two allpass sections 2

ELECTRICAL ENGINEERING

Bernd Jaekel
Coupling between helically twisted wires 7

Ana N. Vučković, Saša S. Ilić, Slavoljub R. Aleksić
Calculation of the attraction and levitation forces using magnetization charges 12

Sergey E. Ryvkin, Felix A. Himmelstoss
Novel switched converter for photovoltaic electricity production (control aspects) 17

Radisa Dimitrijevic, Dragan Tasic, Nebojsa Raicevic, Slavoljub Aleksic, Miodrag Stojanovic, Neda Pekaric-Nadj, Ion Patru
Experimental investigation on MV cables in heating cycle 25

Nenad N. Cvetković
Comparison of two different models for a vertical wire electrode inside a pillar foundation 29

Lenart Kralj, Damijan Miljavec
Nonlinear surface impedance for eddy current losses calculation in power transformer construction parts 34

Vasilija J. Šarac, Dobri M. Čundev
Electromagnetic fields calculation at single phase shaded pole motor 41

Alessandro Fanti, Giuseppe Mazzarella
Vector finite difference approach to the computation of circular waveguide modes 46

Petar Rashkov Penchev
A detailed analysis of Michelson-Morley experiment (MME) 54

Round-off noise calculation in power symmetric filterbank using parallel connection of two allpass sections

Dragana U. Živaljević, Vidosav S. Stojanović

Direct synthesis of recursive digital two-channels filterbanks, whose attenuation characteristic in the passband lies between the Butterworth's and the Elliptic's attenuation characteristics, is described in this paper. Transfer functions with single and multiple zeros on the unit circle are discussed. These transfer functions have arbitrary flatness in the origin and theirs attenuation characteristics have one extremal value in the passband and in the stopband. Complementary decomposition into parallel connection of two allpass filters is performed by separation of poles that lie on the imaginary axis. Next, lowpass filter is obtained by summing these two filters and its complementary highpass filter - by their subtraction. Then, noise produced by multiplication round-off errors and coefficient-quantization effect, is presented. It is shown that introduction of the allpass complementary decomposition significantly reduces the roundoff noise.

Introduction

During the last two decades, power symmetric filter banks have been used in sub-band of speech signals, image processing, multirate signal processing, wavelets and transmultiplexers. Originally, the concept of power symmetric filter banks is introduced for removing aliasing distortion in speech coding. Many design algorithms have been developed to obtain perfect or nearly perfect reconstruction filter banks. Most of these techniques focus on the design of the FIR filter bank that does not suffer from instability and phase distortion [1-3]. However, the resulting filters require a large number of coefficients to meet the magnitude specifications. It is well known that from the aspect of decreasing the number of coefficients, the IIR filter bank is more efficient. Designing an IIR filter that has to meet both magnitude and phase specifications simultaneously is generally difficult [4-9].

Complementary decomposition, among known filters, has been possible only for the Butterworth and the Elliptic filters since only attenuation characteristics with the same number of extrema in the passband and in the stopband can be used. Direct synthesis of a new IIR filter class, whose attenuation characteristic lies in the area between the Butterworth's and the Elliptic's attenuation character-istics of the same order, is proposed in this paper. All poles of the new transfer function are at the imaginary axis and all zeros are on the unit circle. This function satisfies all complementary decomposition conditions and condition for aliasing distortion removing.

Complementary decomposition into parallel connection of two allpass filters is performed. Then, lowpass filter is obtained summing these two filters and its complementary highpass filter - by their subtraction. The main advantage of this kind of filters is smaller sensitivity to digital word length change comparing to standard filters.

In implementing digital filter bank in hardware or software, it is important to consider the finite word-length effects. For example, if a filter is to be implemented on a fixed-point processor, the filter coefficients must be quantized to a finite number of bits. This will change the frequency response characteristics of the filter i.e. filter output is different from the ideal one.

Coefficient-quantization errors introduce perturbations in the zeros and poles of the transfer function which manifest as errors in the frequency response.

Product-quantization errors, on the other hand, can be regarded as noise sources that give rise to output roundoff noise. In performing computations within a fixed- or floating- point digital processor, it is necessary to quantize numbers by either truncation or rounding from some level of precision to a lower level. For example, multiplying two 16-bit fixed-point numbers will produce a product with up to 31 bits of precision so the product will generally need to be quantized back to 16 bits. Round-off noise is introduced into a digital filter when products or sums of

Coupling between helically twisted wires

Bernd Jaekel

The arrangement of conductors in a multi-core power cable leads to a situation where various conductor loops are built up. One or several loops are formed by the phase and neutral conductors with the operational current flowing in these conductors. A further loop is built up by the protective earth conductor which is connected to the equipotential bonding system at several locations. The area of this loop is essentially arranged outside of the power cable. The inductive coupling from the phase conductor loops into that loop causes common mode voltages in the protective earth system with consequent common mode currents. It can be demonstrated that this effect takes place even in case of balanced phase currents in the cable. Numerical simulations and parameter studies were carried out in order to describe this effect quantitatively and to investigate the influence of different cable parameters onto the resulting common mode voltages.

Introduction

Power cables represent components of an entire power supply network which can be carried out in different types. If an earthed system is required, i.e. a system which is connected to the local reference earth, mainly two types of sup-ply networks can be distinguished: TN-C and TN-S. From the point of view of electromagnetic compatibility (EMC) a TN-S power network should definitely be preferred [1]. In this type of network the neutral (N) and protective earth (PE) conductors are strictly separated except at one net point where both conductors are connected, normally at the transformer or the switchgear. This type of installation prevents flowing of any operational currents outside of the phase and neutral conductors. There should be no net currents and therefore the equipotential bonding system is generally assumed to be free of any operational currents. But when looking at this type of network and the physical structure of power cables in more detail some physical mechanisms can be identified which nevertheless lead to generation of common mode voltages and common mode currents even in the case of balanced loaded TN-S power net systems.

Low voltage power cables

Multi-core low voltage power cables consist of the phase conductors and – depending on the grounding arrangement of the power supply network – of a neutral conductor and/or a PE conductor. An example for the structure of a power cable is shown in Fig. 1 for a cable of type NYY. Each of the conductors as well as the entire conductor arrangement are covered by an insulation, for which material is chosen depending on the specific requirements and fields of applications [2].

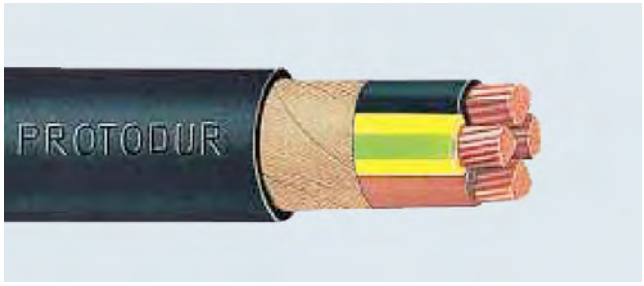

Fig.1. Multi-core power cable of type NYY.

The ***n*** (***n*** = 3, 4 or 5) individual conductors are twisted together and each conductor can be represented by a helical line. An appropriate cylindrical coordinate system for describing the spatial arrangement of a conductor is shown in Fig. 2 together with the relevant parameters: ***a*** as the radius of the helical line with respect to the centre line of the cable and the pitch distance ***p*** as the twist length of the cable, i.e. the length of the cable per rotation of the conductors. For simplicity reasons only one conductor is shown. The further ***n-1*** conductors can be represented as similar lines and they are rotated by an angle $\Phi = 360/n$ with respect to that one shown in Fig.2.

Common mode voltages in power cables

The magnetic flux density **B** caused by the currents in the individual conductors can be calculated by

Calculation of the attraction and levitation forces using magnetization charges

Ana N. Vučković, Saša S. Ilić, Slavoljub R. Aleksić

Calculations of the levitation force between two block permanent magnets and the attraction force that acts between block permanent magnet and infinite linear magnetic plane are presented in the paper. The approach based on magnetization charges is used for those calculations. Results obtained using presented method enable rapid parametric studies of the interaction force relative to material properties, dimensions, and spacing. Obtained expression is easily implemented in any programming environment and requires less than a minute of run time on a personal computer. The results are given in the graphical form. Normalized distributions of magnetic field and magnetic flux density for the system of two permanent magnets are also presented in the paper. Comparing to other methods for interaction force calculation the advantage of presented approach is its simplicity and time efficiency.

Introduction

Permanent magnets of various shapes are often utilized in magnetic actuators, sensors or releasable magnetic fasteners. Knowledge of the magnetic force, either levitation or attraction, is required to control devices reliably [1]. For example, the attraction force exerted between a magnet and a large iron piece, can be obtained by calculating the force between the magnet and its magnetic image. But the main difficulty is to calculate the interaction forces between two different permanent magnets. The calculation of the forces interacting between two magnets can be applied to many other cases (magnetic bearings, attraction systems, etc ...) [2-4].

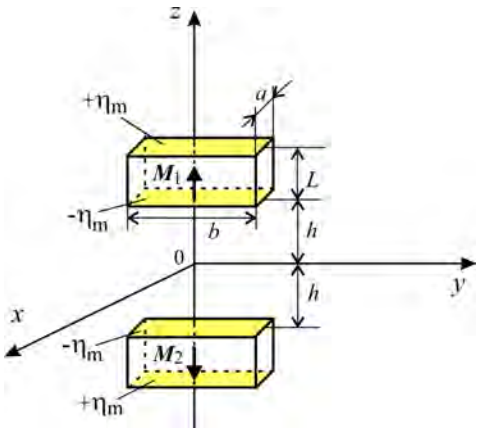

Fig.1. Block permanent magnets.

There are numerous techniques for analyzing permanent magnet devices and different approaches for determining interaction forces between magnets [5-9]. Indeed, the force is the value of importance for design and optimization of a magnetic device. Many authors proposed simplified and robust formulations of the interaction forces created by permanent magnets. The authors generally use the Amperian current model [5-7] or the Coulombian approach [9].

Two different systems are considered in this paper. The first one consists of two identical block permanent magnets made of the same material and magnetized uniformly along the axis of symmetry, but in opposite directions (Fig.1). The second system is composed of block permanent magnet and infinite linear magnetic plane (Fig.2). Levitation and attraction forces are determined using the approach based on magnetization charges [10].

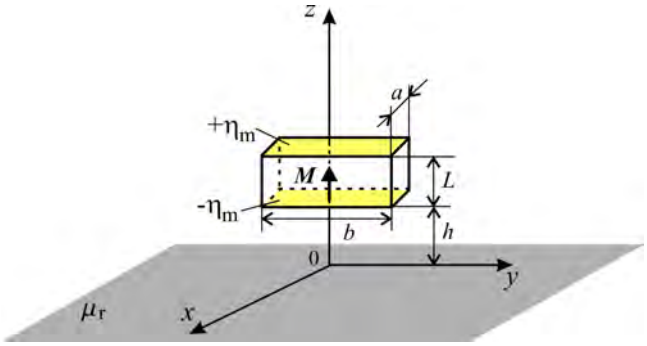

Fig.2. Permanent magnet and infinite linear magnetic plane.

In 1984, Akoun and Yonnet published their expression for calculating the forces between two parallel block magnets with vertical magnetization [11]. More

Novel switched converter for photovoltaic electricity production (control aspects)

Sergey E. Ryvkin, Felix A. Himmelstoss

There are two main tendencies in the nowadays non-carbon based electricity production, distribution and use world. First one is a conversation by electrical power production from conventional, fossil (and short term) based energy sources to renewable energy sources. And connected with it another one: using high efficient power electronics in power generation, power transmission/distribution and end-user application, i.e. step-up-down converters. This paper discusses a new type of such converter that could be used in the low voltages and low power DC drives, e.g. in cars and robots. The main attention is paid to the control problem. The converter behavior is analyzed by using its switching structure model. The model of the drive, the design of the devices, the control features are discussed, feed-forward control based on solving the limit cycle is designed, some experimental results, and hints for the design are given.

Introduction

More 60 % of all energy consumption will be converted and used as electricity, which consumption grows rapidly. It makes a major contribution to global warming [1], [2]. Nowadays emerging climate changes argue to find new effective solutions for reducing this danger. One of the possible ways is a „green electronics“, which involves two major technologies [3]. One is the transferring to such renewable energy sources as wind energy, photovoltaics (PV), and sea wave energy [4] and so on into. The second one is efficient using electrical energy, e.g. using high efficient power electronics in power generation, power transmission/distribution and end-user application. Merge able using both solutions will give synergetic effect and contribute steadily more to non-carbon based electricity production.

However the renewable energy sources have their specifically features that must be take into account. For instance, the solar energy is most abundant energy resource on earth. There is a possibility of the direct conversion of sunlight into electricity by using PV cells. This technology has a particularly promising future. The IEA roadmap emphasizes that by 2050, PV will provide 11% of global electricity production (4500 TWh per year) [2]. In this case there will be together with contributing to significant greenhouse gas emission reductions, substantial benefits in terms of security of energy supply and socio-economic development. However for achieving this advantages the costs of system components (PV modules, DC/AC inverters, cables, fittings and manpower) must be reduced and conversion efficiency of the PV conversion must be and increased. The main merit of the PV cell is that it is an all-electrical device that produces electrical power directly from sunlight and hasn't any moving parts. Therefore, its lifetime could be more than 25 years. However from another side the to-day's PV modules has a light-to-electricity efficiency of no more than 15% and a very large area for the production of the needed end-user application voltage is necessary. E.g. the PV module that usually consists of around 36 or 72 cells connected in series, encapsulated in a structure made of e.g. aluminum, The second demerit of the PV module is the capability reduction to (75~80) % of the nominal rate due to ageing.

For the elimination of the above-mentioned demerits new system components and new control must be designed. One of the possible way solving is using the step-up (boost) converters that transforms the PV output low voltages to the consumer rated voltage. Such converters is equipped with power semiconductor switches, e.g. Insulated-Gate Bipolar Transistors (IGBTs) operating in switch mode with distinctly higher switching frequency, and a capacitor as an additional voltage source [5], [6]. From the control viewpoint such converter is a switched non-linear control plant [7]. Its main feature is that there is only one control, i.e. the transistor one, and two variables: output voltage and capacitor one. This article covers the control aspects of the novel step-up-down converter allowed changing the output voltage in the wide range [8], [9].

Experimental investigation on MV cables in heating cycle

Radisa Dimitrijevic, Dragan Tasic, Nebojsa Raicevic, Slavoljub Aleksic, Miodrag Stojanovic, Neda Pekaric-Nadj, Ion Patru

In order to provide good performance in the service for a long time, power cables shall be developed and designed, including the best materials, available on the market. During exploitation they must withstand combined electrical, thermal and mechanical strengths, such as other influences of environment. Therefore, they must be subjected to some test sequences in order to find out possible behavior in the exploitation. The tests with cycle heating under AC voltage are long-term and the most severe. Measurement of partial discharge on the cable sample is good indication about the stage of cable.

Introduction

When the power cable is finished in the production, it must be subjected to so-called routine test to check, if some latent defect exists. This test is performed on each produced cable length. In the case, when some new cable design is developed or some new important material (for instance, new material for primary insulation) is included in the cable design or simply when a cable manufacturer shall convince his buyer in cable quality, type test must be performed. During this test, cable is subjected to accelerated aging under the influences of raised AC load (current). These may act simultaneously in cycles of intermittent heating and cooling. When this sequence of the test is finished, partial discharge shall be measured for evidence of stage of cable insulation.

Used data

A sample of cable, being tested, shall be 10 m to 15 m long. Two terminations on both cable end shall be assembled, because of strong electrical stresses at the ends of semi conducting screen. Some of the stress relief method must be applied for cable to avoid early electrical breakdown. Heat shrinkable termination is usually used. Cable itself was made of aluminium compacted conductor, XLPE insulation, semi conductive screen over conductor and insulation, insulating swellable tape and laminated Al copolymer foil against longitudinal and radial water penetration and outer sheath of black high density polyethylene.

Some of cable data, such as cable termination data is shown in Table 1. To prevent flashover along the outer surface of cable termination during the impulse voltage test, four rain sheds are shrinked around each termination on both sides to provide safe creepage distance.

Table 1

Design of the cable Al-XLPE/Alfoil/PEwp

Cable			Cable termination	
Conductor	Cross section (mm^2)	150	Type	Outdoor, heat shrinkable
	Material, shape	Al, round	Type of connection	Cable compression type terminal lug, made of Al (could be bimetallic)
	Diameter (mm)	15.1	Type of stress relief	Resistive, stress relief pad – thickness 1 mm
Conductor and insulation screen	Thickness (mm)	0.3	Outer protection	Dual wall HS tube, consisting of outer XLPE layer+inner EPR rubber
XLPE insulation	Thickness (mm)	5.5		
Copper screen (Cu tapes + wires)	Cross section (mm^2)	25	Ground wire	Yes
Aluminium in Al copolymer foil	Thickness (mm)	0.2	Length of cable insulation, covered by stress relief pad (mm)	100
Outer PVC sheath	Thickness (mm)	2.0		
Completed cable	Diameter (mm)	35	Total length approx (mm)	350

Program of Electrical type test

A sample of cable, described in the previous section shall be subjected to the following sequence of tests [1]:

a) bending test, followed by a partial discharge test;
b) tgδ measurement;
c) heating cycle test, followed by a partial discharge test;

Comparison of two different models for a vertical wire electrode inside a pillar foundation

Nenad N. Cvetković

Two different, recently proposed, approaches to modeling the influence of a concrete pillar foundation on grounding characteristics of a wire electrode, which models vertical armature conductors, are presented in this paper. One model is based on modeling the foundation as a cylindrically-shaped semi-conducting inhomogeneity. It provides approximating of the foundation-armature system with one wire of equivalent parameters. The other one considers approximating the foundation with a semi-conducting hemisphere and includes image-theory application and using of Green's function for point source inside hemispherical inhomogeneity. Both approaches include modeling of the armature conductors' system with one wire electrode using complex function theory. are applied for analyzing foundation realized in practice, and the results obtained for the grounding impedance are compared. The quasi-stationary regime is considered.

Introduction

There are many recently published papers dealing with modeling of the pillar foundation influence on pillar grounding system characteristics based on two approaches presented and applied in this paper.

In [1]-[4] foundation is modeled as a semi-conducting hemisphere of known electrical parameters. The applied model considers using a recently proposed approximate expression for the Green`s function of the point source inside/outside of the semi-conducting sphere [5] and the quasi-stationary image theory.

The approach that is based on approximating a wire electrode inside a concrete foundation, modeled as a semi-conducting cylindrically-shaped domain, with a vertical wire electrode of equivalent geometry parameters (length and cross-section dimension) placed in homogeneous earth is presented in [6]-[8].

Common for both approaches is that a single wire conductor inside the foundation is actually an equivalent electrode that models the system of vertical armature electrodes, and that is the way of realizing such systems in practice. Also, the constant leakage current from the electrode is assumed.

The geometry parameters and electrical parameters of the concrete are taken from the official publications, national [9] and international ones [10]-[13]. The results for the impedance obtained using both discussed methods are presented and mutually compared.

Theoretical background

Modelling foundation as a hemispherical domain

A single vertical wire electrode of length l and cross-section radius a is placed inside a semi-conducting hemisphere having radius r_s, of known electrical parameters σ_s, ε_s, whereas surrounding ground parameters are σ_1, ε_1, Fig.1. The electrode is fed by a LF current, I_g. Single electrode is actually a model of the wire armature cage formed of N parallel conductors of length l, having a circular cross-section of radius r_0, (upper part of Fig.1). Applying the procedure based on using a complex function (which can be found in [2] and [6]), a system of vertical armature electrodes is replaced by a single wire electrode having cross-section of radius a placed in the concrete foundation. Length of a single equivalent electrode is l and $a = a_1 \sqrt[N]{N\, r_0 / a_1}$ is the equivalent radius of circular cross-section [2], [7].

The applied procedure for determining the electric scalar potential in the vicinity of the electrode from Fig.1 considers using recently proposed Green's functions for the point source inside/outside hemispherical inhomogeneity [2]. Since the results for resistance of the electrode from Fig.1 will be

Nonlinear surface impedance for eddy current losses calculation in power transformer construction parts

Lenart Kralj, Damijan Miljavec

The article deals with the use of nonlinear surface impedance for the eddy current losses calculation in a power transformer tank walls and other electrically conductive construction parts. The aim of this analyze was also to calculate the electric and magnetic field distribution into the depth of tank wall. These results are used to confirm the correct definition and use of nonlinear surface impedance. A comparison between the calculated losses using linear and nonlinear surface impedance is demonstrated. A time harmonic 3D finite element method is used to compute the magnetic leakage fields in the surroundings of analyzed power transformer. The simulations are validated by using the measuring results based on the short circuit method.

Introduction

Linear and nonlinear surface impedance is used to present the conductive construction parts of power transformer, such as tank walls, yoke clamps and other construction parts. The surface impedances are applied to calculate the eddy current losses in described construction parts. The sources of eddy current losses are due to leakage magnetic fields. The 3D geometric model of power transformer was made and linked with finite element method. The time harmonic analyze is used to investigate the discussed problem. On this basis, we calculated the leakage magnetic field around the three phase primary and secondary coils at nominal current loadings. The analysis was conducted on a previously measured power transformer. Using the measured results, the accuracy of the calculation method was verified and validated. Accurate calculations of these losses in a power transformer based on numerical model may also improve transformer structure in terms of reduced losses and increased overall efficiency [1]-[4].

3-D model of power transformer

The 3D finite element model (Fig.1) is made based on dimensions of real power transformer from the company Etra 33, Slovenia. All the numerical calculations of magnetic fields and eddy current losses were done by commercial software package Cedrat Flux 3D [5].

The electric connections between the coils and the tank wall insulator as well as limb clamps were not taken into account. The limb clamps (between the core and the windings) are made from stainless steel and due to this; they are not presenting a significant source of stray losses and are not included in the analyze. The windings are not described by finite elements, but with current loops (conductors) of prescribed dimensions. The current density is uniform over the cross section of the winding conductors. Regarding the use of non-meshed windings the reduced magnetic scalar potential can be engaged in solving the magnetic fields. The distribution of magnetic fields in the transformer tank (oil) is calculated from Biot-Savart's law and it is presented in Fig.2.

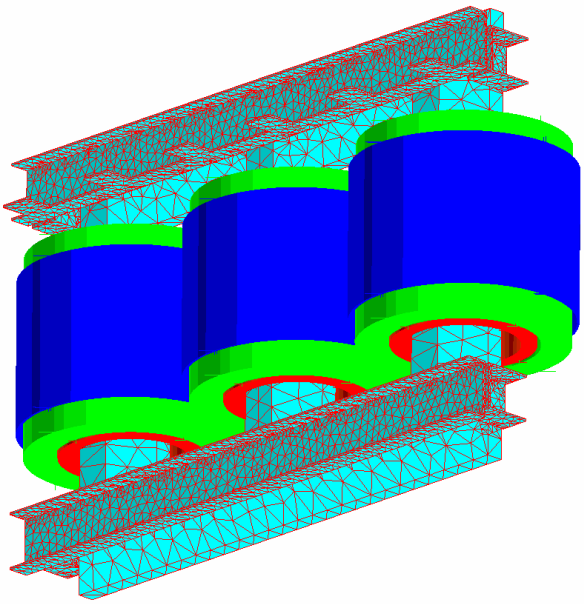

Fig.1. 3-D Finite element model of power transformer.

Electromagnetic fields calculation at single phase shaded pole motor

Vasilija J. Šarac, Dobri M. Čundev

Finite Element Method (FEM) is used for calculation of electromagnetic field inside the single phase shaded pole motor, product of company Micron-Tech from Prilep under trade name AKO-16. Four different motor models for FEM application are developed. In first motor model magnetostatic approach for electromagnetic field calculation is implemented, meaning all electromagnetic quantities are evaluated at zero Herz frequency. Second model is developed using time-harmonic approach at fifty Herz frequency. Third and fourth motor model are developed by implementing soft magnetic material in stator notch and pole respectively and analyses is carried out in time harmonic domain. Obtained results are compared and conclusions are derived.

Introduction

In spite of its simple construction single phase shaded pole motor (SPSPM) is very complex due to the existence of three magnetically coupled windings which produce an elliptic rotating magnetic field in motor's air gap. Motor's prototype rated data are: U_n=220 V, f_n=50 Hz, I_{1n}=0.125 A, P_{1n}=18 W, n_n=2520 rpm and 2p=2 (Fig.1).

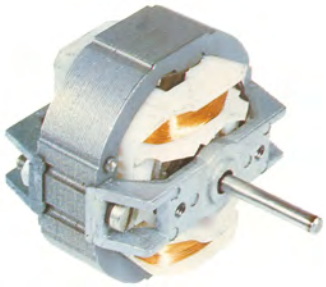

Fig.1 Prototype of motor AKO-16.

Extensive analysis of motor performance characteristic is implemented and they are calculated on the base of symmetrical components theory [1], [2]. Obtained characteristics are verified by experiment [3]. Next step in motor research is to calculate electro-magnetic characteristics such as magnetic flux density inside the motor cross section. Therefore Finite Element Method was employed as valuable tool in calculation of motor electro-magnetic characteristics [4].

FEM motor models

Over the past years Finite Element Method has proved itself as valuable tool in motor design and analysis. In order to enable FEM calculation to be applicable, exact motor geometry with material characteristics is input in FEM pre processing part. Very important issue is to define boundary conditions on outer motor geometry and in this case Dirichlet boundary conditions are used. Another important subject in motor modeling is defining the mesh of finite elements. By dividing the motor's cross section into large number of regions i.e. elements with simple geometry (triangles) the true solution of magnetic vector potential is approximated by a very simple function. Two different approaches are used in magnetic field calculation: magneto-static and time-harmonic [5]. In magneto-static approach all electromagnetic phenomena inside the motor are analyzed in certain moment of time i.e. f=0 Hz. First, motor model is built by inputting current density in main stator winding, than from the value of magnetic flux in short circuit coil, current in the coil is calculated and input in the model. Finally having the both stator currents and from the value of magnetic flux in motor air gap, current in rotor squirrel cage winding is calculated. Having all three currents in the model the program is run at stator frequency f=0 Hz. In time-harmonic motor model only stator current is input and consequently currents in short circuit coil and rotor windings are freely induced. On that way analysis of electromagnetic phenomena inside the motor is closer to the real electromagnetic process inside the machine when it is supplied with voltage 220 V, 50 Hz. Both analyses are performed in 2D domain. Further improvement in motor design is achieved with implementation of soft magnetic powders in motor construction. On that way, rather high value of motor magnetic flux density in time-

Vector finite difference approach to the computation of circular waveguide modes

Alessandro Fanti, Giuseppe Mazzarella

We describe here a Vector Finite Difference approach to the evaluation of waveguide eigenvalues and modes for circular wave guides. The FD is applied using a 2D polar grid, in the waveguide section. A suitable Taylor expansion of the vector mode function, allows to take exactly into account the boundary condition. The FD approximation results in a constrained eigenvalue problem, that we solve using a decomposition method. This approach has been evalutated comparing our results to the analytical modes of the circular waveguide.

Introduction

Circular waveguides are the most popular waveguide structures after rectangular ones [1].

Circular waveguides have been used both as guiding structures, and in different applications as components in waveguide circuits.

In many applications, the knowledge of both eigenvalues and field distributions of waveguides modes are required. Among them, there are the analysis of waveguide junction using mode matching [2], [3] and the solution of waveguide problems with sources [4]. The same type of information is also required in the analysis, using the method of moments (MoM), of thick-walled apertures. Indeed, these apertures can be considered as stub waveguides, and the modes of these guides are the natural basic functions for MoM [5].

There are many different numerical techniques that have been proposed to evaluate the mode vector in a waveguide. In particular, the Finite Difference approach (FD), [6], i.e., the direct discretization of the eigenvalue problem, is the simplest strategy, but is a very effective solution only for rectangular waveguide, since only in these case the boundary is perfectly fitted to the discretization grid.

Of course, for a circular waveguides standard [7] FD require a very fine mesh to approximate the boundary. Therefore in [8], use of a polar grid has been proposed. Since the boundary is exactly represented, use of a polar grid allows accurate results to be obtained with a course mesh. A drawback of existing FD approach is that all of them compute the eigenfunctions of Hertz potential, though the basis functions of MoM are the vector eigenfunctions. Starting with the Hertz potential, a numerical derivative is therefore required, which can results in reduced accuracy.

Aim of this work is to present the direct computation of vector eigenfunctions in a waveguide, using a finite difference (FD) [9], [10] approximation of the vector Helmholtz equation [11], [12], [13], [14] on a polar grid [8]. Since we are mainly interested in using those modes in MoM, the entire development will be expressed in term of equivalent magnetic surface currents [15]. For each internal grid point, a second order Taylor approximation allows to evaluate the surface magnetic current in the neighboring points. In this work we use a vector generalization of FD approach presented in [16]. This leads to a matrix eigenvector problem, when suitable conditions are added. These come out from the boundary condition and the solenoidal or irrotational condition on mode vectors [17]. The constrained eigenvalue problem can then be solved using linear algebra tecniques [18]. The resulting techniques gives results comparable to those obtained with FEM and FIT techniques, but with a lower computational cost.

Description of the technique

Let use consider a circular waveguide. The TE modes $\vec{e}$ is an eigenfunction of the Helmholtz equation:

$$(1) \qquad \begin{cases} \nabla_t^2 \vec{e} + k_t^2 \vec{e} = 0 \\ \nabla_t \cdot \vec{e} = 0 \\ \vec{e} \times \vec{i_n}\big|_C = 0 \end{cases}$$

where C is the contour of the waveguide (see Fig.1).

A detailed analysis of Michelson-Morley experiment (MME)

Petar Rashkov Penchev

This paper presents an analysis of the significant for physics Michelson-Morley experiment, MME, as to why there is no interference despite its theoretical setup, which requires interference. The analysis demonstrates that there is a flaw in the setup of the experiment and therefore it groundlessly requires interference. This flaw corrected, the theoretical setup of MME no more requires interference, as MME demonstrates itself. Under these conditions, there is no more need for Lorentz's postulate of shortening one arm of Michelson interferometer in order to explain why there is no interference.

1. Introduction

So far, no one has presented a real experimental proof of H. Lorentz's postulate of shortening the length ℓ_0 of bodies in direction of the velocity v of motion of $\ell = \ell_0 \cdot \sqrt{1-\frac{v^2}{c^2}}$, (where $\boldsymbol{c}$ is the velocity of light). And this postulate is the key to the explanation of the experimental fact that there is no interference in Michelson-Morley experiment (MME) .

It is a fact that Lorentz's postulate[1] of shortening the bodies has no experimental proof even today, over a hundred years later; on the contrary, there are facts which contradict it and its corollaries. This has motivated the author to question Lorentz's postulate and the inference that the postulate is fully reliable, i.e. to ask whether Lorentz's interpretation of the MME results is incorrect or the theoretical setup of MME is flawed.

2. Basic initial assumptions in MME

The earth *(Z)* moves along its orbit around the sun at velocity $v_Z = 30\ \text{km.s}^{-1}$. At the same time, the earth surface moves around its axis at velocity $v_{Z0} = 0{,}5\ \text{km.s}^{-1}$. Since v_{Z0} is ignorably low compared to v_Z, it is assumed that all points on the earth (*Z*) move along its orbit at velocity $v_Z = 30\ \text{km.s}^{-1}$, relative to point O_Z of reference frame K_Z in fig. 1, which point lies on its orbit (assumed to be a linear part) around the sun. In this sense, axis *r* in the diagram of the earth *(Z)* along its orbit is assumed as its orbit.

In this sense point O_Z (fig. 1) is assumed as starting point of distance r_Z, covered by the earth *(Z)* travelling at velocity v_Z for time t along its orbit, which is $r_Z = v_Z.t$, as well as the velocity v_Z.

The diagram of MME with the Michelson interferometer, positioned immovably on the surface of the earth is given in fig. 2, where is given part of the surface S_Z of the earth, designated by the closed curve *L*.

The reference frame for the velocities of the light pulses in MME is designated by K_0, and the beginnings of its axes coincide with the beginning O_0 of the arms $\overline{O_0A_1}$ and $\overline{O_0B_1}$ of the interferometer. The arms $\overline{O_0A_1}$ and $\overline{O_0B_1}$ are perpendicular to each other and have equal lengths $\ell_A = \ell_B = \ell_0$. At their ends A_1 and B_1, the arms have reflecting mirrors for the light pulses. *G* is the generator of light pulses and it is fixed to the beginnings O_0 of the arms $\overline{O_0A_1}$ and $\overline{O_0B_1}$. The semitransparent prism (lamella), positioned at the beginning O_0 of the arms divide the light pulse into two reciprocally perpendicular beams along the two arms. The reflecting mirrors at the ends of arms A_1 and B_1 return the beams to O_0, after which the beams converge into the observation device *S*.

The interferometer (fig. 2) is mounted immovably on the surface of the earth (*Z* – fig. 1, respectively fig. 2) and therefore its velocity v_Z relative to the earth *(Z)* is zero $v_i = 0$. And the velocity of the interferometer (the arms of the interferometer) relative to the reference frame K_Z (fig. 1) with reference starting point O_Z is equal to the velocity of the earth *(Z)*, which is v_Z along its orbit (fig. 1), since the interferometer is fixed

[1] The meaning of the word postulate, according to the Bulgarian Academy of Sciences Interpreting Dictionary of Foreigh Words in the Bulgarian Language, is "an initial assumption accepted without experimental proof".